Probabilistic Stability Analysis of an Embankment on Soft Clay

H. El-Ramly, AMEC Earth and Environmental, Edmonton, AB, Canada
N.R. Morgenstern, and D.M. Cruden, Department of Civil and Environmental Engineering, University of Alberta, Edmonton, AB, Canada

ABSTRACT
A probabilistic slope analysis methodology based on Monte Carlo simulation using Microsoft Excel and @Risk software is applied to study the performance of the Muar trial embankment in Malaysia. The study demonstrates the techniques used in quantifying the various sources of uncertainty associated with the undrained shear strengths of clay foundations, and estimating the probability of unsatisfactory performance. The relationships between embankment height, factor of safety and probability of unsatisfactory performance at different stages during construction are examined. Sensitivity analyses show that the uncertainties in Bjerrum's vane correction factor and the contribution of embankment fill strength to stability have significant impacts on the reliability of the factor of safety.

RÉSUMÉ
La performance d'un remblais d'essai à Muar, en Malaisie, est évaluée avec une méthode d'analyse probabiliste qui incorpore la simulation Monte Carlo comme base, et utilise les logiciels Microsoft Excel et @Risk. L'article démontre les techniques suivis pour quantifier les sources d'incertitudes reliées à l'estimation de résistance au cisaillement des matériaux de fondations et à l'estimation de la probabilité d'obtenir une performance insatisfaisante. La relation entre hauteur de remblais, facteur de sécurité et probabilité de performance insatisfaisante durant différents niveaux de construction est examinée. Des analyses de sensibilité démontrent que la fiabilité du facteur de sécurité est fortement affecter par certain incertitudes telles que ; le facteur de correction scissométrique de Bjerrum et par la contribution à la résistance du matériel de remblais.

1. INTRODUCTION

Despite decades of accumulated experience, the ability of the geotechnical profession to make reliable forecasts of slope failures remains poor. As an example, in 1989 the Malaysian Highway Authority built a full-scale trial embankment in the valley of the Muar River to optimize the design of a highway embankment on soft marine clay. A detailed soil investigation program was conducted, and extensive amounts of data were collected. Prior to construction, thirty geotechnical consultants were invited to predict the performance of the trial embankment, including its height at failure. Brand and Premchitt (1989) and Poulos et al. (1990) provided a discussion of the predictions and the results of the field trial. The embankment failed when the thickness of the placed fill reached 5.4m. At the time of failure the average settlement of the embankment was about 0.7 m, and the height of the embankment above average ground was 4.7 m. Figure 1 is a histogram of predictions of embankment height at failure. A significant scatter in the predictions is evident, even though all participants had the same site characterization data.

The difficulties in predicting field performances in geotechnical engineering are attributed to the substantial uncertainties that dominate the profession. Probabilistic techniques offer an attractive framework for quantifying and incorporating uncertainty in slope analysis and design.

The stability of the Muar embankment is analysed using the probabilistic methodology by El-Ramly et al. (2002a), and the conventional approach based on the factor of safety. The relationships between embankment height at various stages during construction and the probability of unsatisfactory performance (or failure probabilities) and factor of safety are examined. The study is one of a series of case histories (El-Ramly et al., 2002a; 2002b; 2003a) illustrating the value of probabilistic techniques, and providing guidelines for acceptable probabilities of unsatisfactory performance.

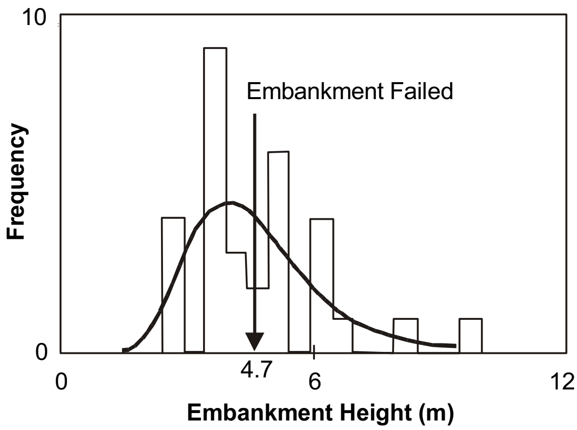

Figure 1 Histogram of predictions of embankment height above ground at failure (modified from Kay, 1993).

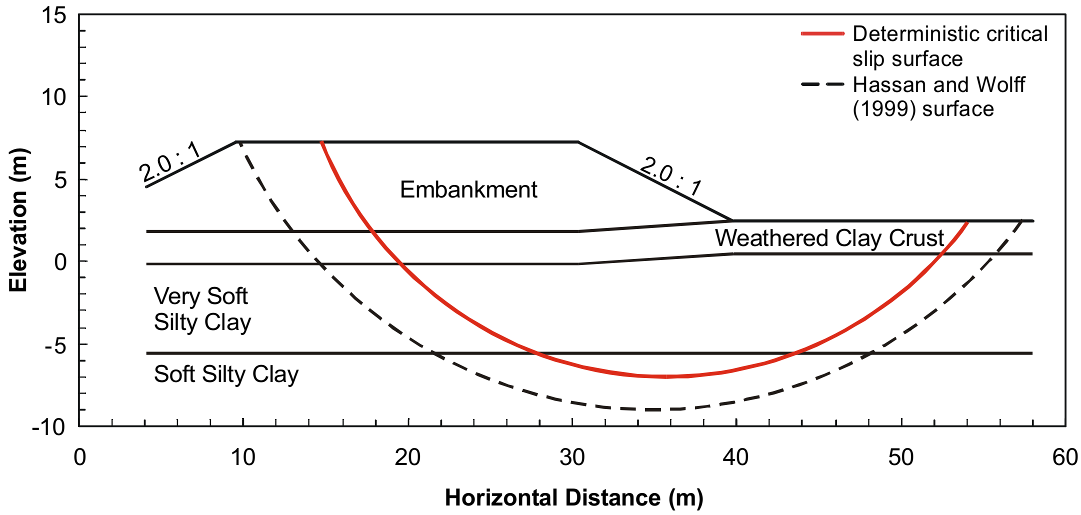

Figure 2 Geometry and stratigraphy of the Muar embankment at failure

2. STRATIGRAPHY AND SOIL CHARACTERISTICS

The Muar Trial embankment had a base area of about 55 m x 90 m and side slopes of 2h:1v; a cross-section of the embankment is shown in Figure 2. It was constructed on a crust of weathered clay, about 2.0m thick, underlain by very soft to soft clays. Two clay layers of different properties were identified. Immediately below the weathered crust, 6.0 m of highly plastic, very soft clay were encountered followed by 9.5 m of soft clay of lower plasticity and slightly higher strength. The clay sequence was underlain by 0.7 m of peat on top of dense clayey sand. Figure 3 shows soil stratigraphy and Table 1 summarizes the physical and mechanical characteristics of clay layers. Detailed descriptions of the geology and soil conditions are given in the report prepared by the Asian Institute of Technology (AIT, 1989) and the summary paper by Brand and Premchitt (1989).

The undrained shear strengths of subsurface soils were assessed through 9 field vane soundings. Figure 3 shows the variation of the undrained shear strength with depth. The strength of the desiccated crust is much higher than that of the underlying very soft clay, and decreases from about 50 kPa at surface to 8 kPa at 2 m depth. The strengths of the underlying clay layers increase almost linearly with depth from about 6.5 kPa at 2 m below surface to 34 kPa at 17 m depth.

3. SOURCES OF UNCERTAINTY

Construction of the embankment took 100 days and, hence, undrained conditions prevailed at failure. The stability of the embankment is governed by the undrained shear strength of foundation soils, and the shear strength of embankment fill. Uncertainties in shear strength parameters are attributed to the inherent spatial variability of the soil layers, and systematic sources of uncertainty including biases in empirical factors used in deducing strength values and statistical uncertainties due to limited amounts of data available. In the following sections, uncertainties in input parameters whose impacts on the stability of the embankment could be significant are quantified.

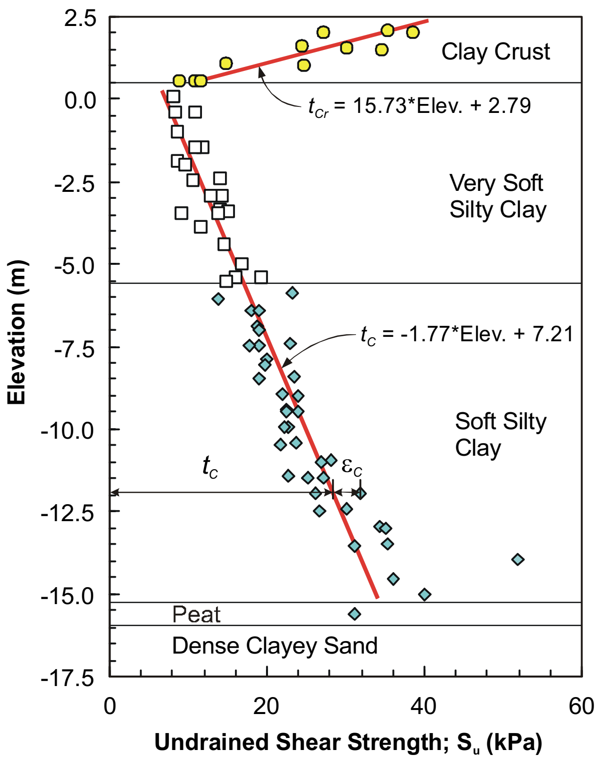

Figure 3 Profile of field vane shear strength

Table 1. Summary of soil properties of clay layers

Soil Layer	LL (%)	PL (%)	LI (%)	e	γ_b (kN/m^3)
Clay Crust	90	30	0.6	1.85	15.5
Very Soft Silty Clay	80	27	1.5	2.60	14.0
Soft Silty Clay	55	23	1.4	1.65	16.0

LL, liquid limit; PL, plastic limit; LI, liquidity, index; e, void ratio; γ_b, bulk unit weight.

3.1 Very Soft and Soft Clay Layers

Figure 3 shows hardly any distinction between the undrained shear strengths of the very soft and the soft clay layers in terms of trend and scatter of measurements. Hence, the data of the two layers are combined and the undrained shear strengths are treated as one population. It should be noted that this approximation does not reflect the geology on site as indicated by the different physical properties of the two layers (Table 1). It is only a modelling approach to simplify the statistical treatment of the data. The validity of this simplification is examined in the following paragraphs. For illustration purposes, all parameters pertaining to the subject clay layers are identified with a "$_C$" subscript.

The undrained shear strength of the clays is considered a random variable and modelled using Equation 1,

$$S_{u\text{-}C} = \mu_C\, S_{u\text{-}M} = \mu_C\,(t_C + \varepsilon_C) \qquad [1]$$

where $S_{u\text{-}C}$ is the undrained shear strength at location i, μ_C is Bjerrum's vane correction factor (Bjerrum, 1972), and $S_{u\text{-}M}$ is the measured vane strength at the same location. The measured vane strength is divided into a trend component, t_C, dependent on location, and a residual component, ε_C, that characterizes the spatial variation of strength over and above the trend value, as shown in Figure 3.

Using the method of least squares, a linear trend is fitted to the vane data (Figure 3). The mean values of the slope, $E[a_{1\text{-}C}]$, and intercept, $E[a_{o\text{-}C}]$, of the trend line are -1.77 kPa/m and 7.21 kPa, respectively. Since $E[a_{1\text{-}C}]$ and $E[a_{o\text{-}C}]$ are estimated based on a limited amount of data, they are also uncertain. Assuming $a_{1\text{-}C}$ and $a_{o\text{-}C}$ are normally distributed random variables, statistical theory (Neter et al. 1990) allows estimating the variances $\sigma^2[a_{1\text{-}C}]$ and $\sigma^2[a_{o\text{-}C}]$ as follows;

$$\sigma^2[a_{1\text{-}C}] = \frac{\sigma^2\left[S_{u\text{-}M}\right]}{\sum (z_i - E[z])^2} \qquad [2]$$

$$\sigma^2[a_{o\text{-}C}] = \sigma^2\left[S_{u\text{-}M}\right]\left\{\frac{1}{n} + \frac{E[z]^2}{\sum (z_i - E[z])^2}\right\} \qquad [3]$$

where E[-] and σ^2[-] are the mean and variance, respectively, z_i is the depth, and n is the number of vane measurements. The estimates $a_{1\text{-}C}$ and $a_{o\text{-}C}$, are usually correlated. The correlation coefficient $\rho(a_{1\text{-}C}, a_{o\text{-}C})$ is given by;

$$\rho(a_{o\text{-}C}, a_{1\text{-}C}) = -\frac{E[z]\,\sigma^2[a_1]}{\sigma[a_o]\,\sigma[a_1]} \qquad [4]$$

where σ[-] is the standard deviation. Using Equations 2 through 4, the standard deviations $\sigma[a_{1\text{-}C}]$ and $\sigma[a_{o\text{-}C}]$ are 0.07 kPa/m and 0.63 kPa, respectively, and the correlation coefficient $\rho(a_{1\text{-}C}, a_{o\text{-}C})$ is 0.86.

The trend component is removed from all vane measurements to estimate the statistical population of the residual component ε_C. The residual component has a constant mean of zero and a standard deviation, $\sigma[\varepsilon_C]$, of 2.45 kPa. Figure 4 shows the histogram of ε_C. It exhibits a single peak indicating that vane shear strengths of the two clay layers are consistent in a statistical sense.

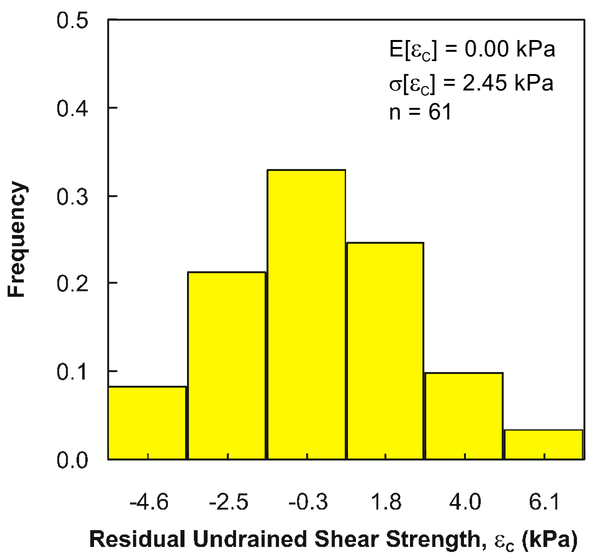

Figure 4 Histogram of residual component of undrained shear strength of clay layers; ε_C

Based on a review of several embankment and cut slope failures, Bjerrum (1972, 1973) recommended applying an empirical correction factor, μ, to vane measurements

(Equation 1) depending on the plasticity index. Figure 5 shows Bjerrum's database, as well as additional cases compiled by Aas et al. (1986). The scatter of the data around Bjerrum's recommended relationship is substantial. Hence, the uncertainty surrounding the vane correction factor is significant and should be addressed in any probabilistic assessment.

Figure 5 indicates a relatively uniform scatter of data points around Bjerrum's mean curve, irrespective of the plasticity index. So, the vane correction factor can be considered a random variable with a mean equal to Bjerrum's recommended curve and a constant standard deviation deduced from the scatter of data around the mean curve. Assuming μ to be normally distributed, the standard deviation $\sigma[\mu]$ is 0.15. Based on the plasticity indices of the subject clay layers, the mean value of Bjerrum's vane correction factor, $E[\mu_C]$, is estimated to be 0.80.

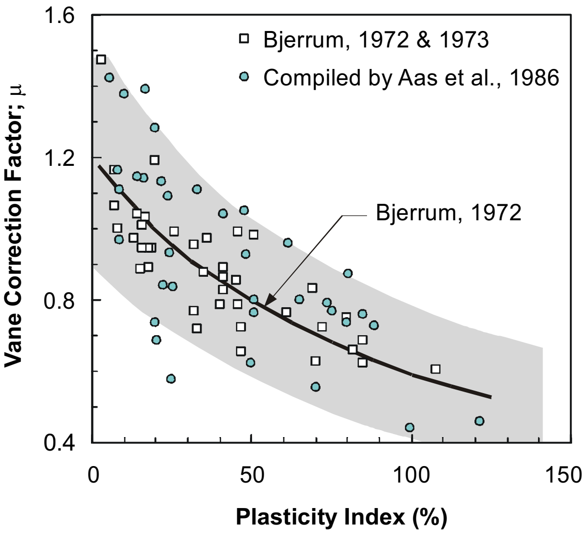

Figure 5 Bjerrum's vane correction factor

3.2 Clay Crust

Published studies (e.g. Lefebvre et al., 1987) suggested that the field vane overestimates the operational shear strength of overconsolidated clay crusts due to the presence of pre-existing fissures. Ferkh and Fell (1994) recommended the use of a reduced strength for the crust. Preliminary slope stability analyses of the Muar embankment using an upper strength threshold of 14 kPa for the weathered crust showed minimal impact, less than 4 percent, on the factor of safety. Hence, no threshold is applied to the measured vane strength of the clay crust.

A similar approach to that in Section 3.1 is used to quantify the uncertainties in the undrained shear strength of the clay crust. For clarity, all parameters pertaining to the clay crust are denoted with a "$_{Cr}$" subscript. A linear trend is fitted to the vane data as shown in Figure 3. The mean values of the slope and intercept, $E[a_{1\text{-}Cr}]$ and $E[a_{o\text{-}Cr}]$, are 15.73 kPa/m and 2.79 kPa, respectively. Assuming normal distributions, the standard deviations, $\sigma[a_{1\text{-}Cr}]$ and $\sigma[a_{o\text{-}Cr}]$, are 2.49 kPa/m and 3.62 kPa. The correlation coefficient $\rho(a_{1\text{-}Cr}, a_{o\text{-}Cr})$ is -0.92. Removing trend values from vane measurements, the mean and standard deviation of the residual component, ε_{Cr}, are zero and 4.55 kPa. Figure 6 shows the histogram of the residual component. The uncertainty in Bjerrum's vane correction factor is represented by a normal probability distribution with a mean of 0.75 (Figure 5) and a standard deviation of 0.15.

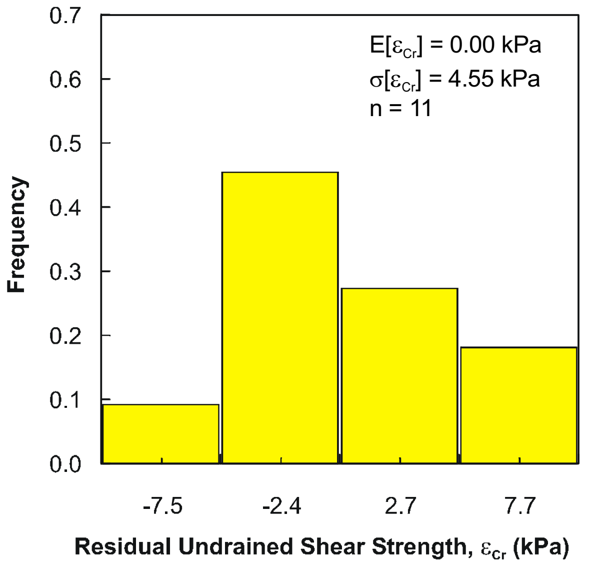

Figure 6 Histogram of residual component of undrained shear strength of clay crust; ε_{Cr}

3.3 Embankment Fill Material

The embankment was constructed using compacted clayey sand to sandy clay fill. As part of the site investigation program, three unconsolidated undrained triaxial tests were performed on samples of fill material. The tests yielded undrained shear strength envelopes with cohesion intercepts ranging between 64 and 19 kPa, and corresponding friction angles ranging between 12 and 26 degrees. An approximate estimate of fill strength is obtained by averaging shear strengths corresponding to a confining stress equivalent to mid height of the embankment from failure envelopes of three triaxial tests. It is estimated to be 60 kPa.

The uncertainty in the operational shear strength of embankment fill is attributed to two factors. First, the procedure used above to estimate the average shear strength is approximate, particularly since the initial stresses within the embankment are not geostatic and depend largely on the compaction energy. Second, the strains experienced by the compacted fill, due to the distortion of the underlying soft clay, exceeds the strain levels at peak strength. Hence, the operational shear strength of the fill at failure is an unknown value between the peak and residual strengths. In the stability analyses in the following sections, the average shear strength of embankment fill along the slip surface is considered a random variable and modelled using a normal probability distribution with a mean equal to 60 kPa. The standard deviation is assigned, judgementally, a value of 12 kPa; a coefficient of variation of 0.2.

4. PROBABILISTIC SLOPE ANALYSIS

4.1 Probabilistic Methodology and Input Variables

The stability of the Muar embankment at failure is analysed using the probabilistic methodology developed by El-Ramly et al. (2002a). Only brief descriptions of the methodology are provided here and the reader is referred to the original paper for more details.

The probabilistic methodology is spreadsheet-based and makes use of the Microsoft Excel (Microsoft, 1997) and @Risk (Palisade, 1996) software. The embankment geometry, stratigraphy, soil properties, critical slip surface(s), and selected method of slope analysis are modelled in an Excel spreadsheet. The Bishop method of slices (Bishop, 1955) is used in the spreadsheet. Three input parameters are considered random variables; the shear strength of the embankment fill, and the undrained shear strengths of the clay crust and the underlying soft clays. Using @Risk functions, each of these input parameters is assigned appropriate probability distributions. To account for the various sources of uncertainty addressed in Section 3, each parameter is represented by a number of variables. The uncertainties due to the spatial variability of clay layers are represented by the observed probability distribution functions of the residual components, whose histograms are shown in Figures 4 and 6. The biases in Bjerrum's vane correction factors and the statistical uncertainties in regression coefficients of the linear trends of the undrained shear strengths are represented by normal probability distributions with the means and standard deviations estimated in Section 3. The correlations between slopes and intercepts of trend lines are established in the spreadsheet using @Risk tools. Table 2 summarizes the statistical parameters of all input variables.

4.2 Autocorrelation Distance and Spatial Variability

To account for the spatial variability of undrained shear strengths along the slip surface, an estimate of the autocorrelation of in-situ soils is required. In the absence of adequate data to conduct a site specific assessment, empirical estimates of horizontal and vertical autocorrelations distances are made based on typical values in the literature (El-Ramly et al., 2003). A range of 30-40 m is postulated as a possible range for the horizontal autocorrelation distance and 1-3 m as a possible range for the vertical autocorrelation distance. To simplify the analysis of spatial variability, an equivalent isotropic autocorrelation distance, rather than different horizontal and vertical distances, is adopted. Using the approximate procedure proposed by El-Ramly (2001) and the typical ranges above, the equivalent isotropic autocorrelation distance, r_o, of the marine clays in the foundation is in the range of 5-15 m. The probabilistic analyses in the following sections are based on an intermediate value of 10 m. The sensitivity of the outputs to the autocorrelation distance is investigated in a latter section.

The spatial variability of the residual components of undrained shear strengths along the slip surface is modelled using one-dimensional, stationary random fields (Vanmarcke, 1983). At any given location along the slip

Table 2. Statistical parameters of input variables

Input variable			Soil spatial variability			Systematic uncertainty		
			E[--]	σ[--]	PDF	E[--]	σ[--]	PDF
Embankment fill; $S_{u\text{-Fill}}$ (kPa)			60.0	12.0	N.	--	--	--
Weathered clay Crust	Trend	$a_{1\text{-Cr}}$ (kPa/m)	--	--	--	15.73	2.49	N.
		$a_{o\text{-Cr}}$ (kPa)	--	--	--	2.79	3.62	N.
	Residuals; ε_{Cr} (kPa)		0.00	4.55	Exper. (Figure 6)	--	--	--
	Bjerrum factor; μ_{Cr}		--	--	--	0.75	0.15	N.
Very soft/soft clay layers	Trend	$a_{1\text{-C}}$ (kPa/m)	--	--	--	-1.77	0.07	N.
		$a_{o\text{-C}}$ (kPa)	--	--	--	7.21	0.63	N.
	Residuals; ε_C (kPa)		0.00	2.45	Exper. (Figure 4)	--	--	--
	Bjerrum factor; μ_C		--	--	--	0.80	0.15	N.

Note: E[-], mean; σ[-], standard deviation; PDF, probability density function; a_1 and a_o, slope and intercept of linear trends of undrained shear strengths; ε, residual component; Exper., experimental probability distribution; N, normal probability distribution.

surface, the residual component ε_C, for example, is a random variable, spatially correlated with the residual components at adjacent locations. Instead of modelling the point-to-point variation of the residual component, the variability of its local averages over local domains within the random field is considered (Vanmarcke, 1983). The portion of the slip surface within each soil layer is divided in the spreadsheet (using principles of analytical geometry) into segments of lengths l_i. The statistical characteristics of local averages of ε_C include the reduction in variance due to spatial averaging and the correlation coefficients between averages over adjacent segments of the slip surface. By taking segment lengths l_i equal to or less than the scale of fluctuation, δ, the variances of local averages approach the point variance and the correlation coefficients between most of the local averages approach zero (Vanmarcke, 1977 and; 1983). Assuming the spatial structure of the residual components follows an exponential autocovariance function, the scale of fluctuation, δ, is equal to twice the autocorrelation distance; approximately 20 m.

4.3 Critical Slip Surface

Two candidate critical slip surfaces are considered; the deterministic critical slip surface based on mean values of input parameters, and the surface corresponding to the minimum reliability index based on the Hassan and Wolff (1999) algorithm (Figure 2). Preliminary Monte Carlo simulations indicated that the probability of unsatisfactory performance associated with the former is higher than that of the latter. Hence, the deterministic critical slip surface is considered the critical surface for probabilistic slope stability analyses.

4.4 Monte Carlo Simulation

Having completed the spreadsheet, Monte Carlo simulation is performed with @Risk drawing at random a value for each input variable from its defined probability distribution. In sampling the input probability distributions, the correlations between variables are maintained. The sampled input values are used to solve the spreadsheet and calculate the corresponding factor of safety. The process is repeated sufficient times to estimate the statistical distribution of the factor of safety. Using 10,000 iterations, the mean and standard deviation of the factor of safety are estimated to be 1.11 and 0.15, respectively. The probability of unsatisfactory performance P_u (probability of factor of safety less than one) is estimated to be $23.8\text{x}10^{-2}$. Figure 7 shows the histogram of the factor of safety. Since the simulation process is based on random sampling of input variables, the calculated probability of unsatisfactory performance is also a variable. Based on the results of 25 simulations (using different seed values), the mean probability of unsatisfactory performance is $24.1\text{x}10^{-2}$. The reliability index, another probabilistic safety indicator, is given by $\beta=\{E[FS]-1\}/\sigma[FS]$, where E[FS] and σ[FS] are the mean and standard deviation of the factor of safety. It is computed to be 0.72.

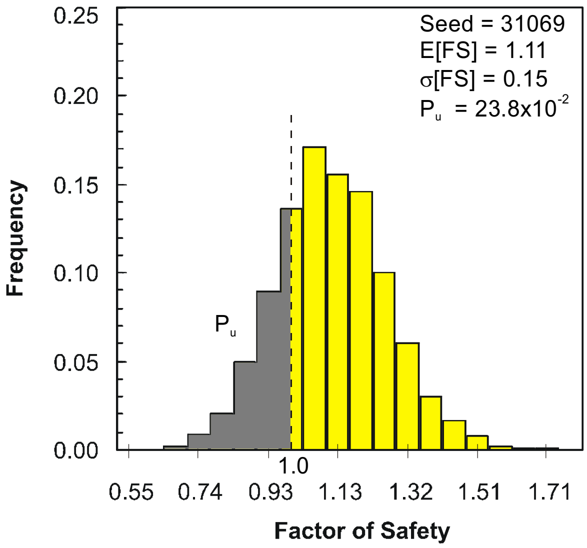

Figure 7 Histogram of factor of safety at failure (embankment height above ground = 4.7 m)

4.5 Calibration of Probability Figures

Providing a link between current slope design practice and probabilistic slope stability analyses is essential in explaining the meanings of the computed probabilities of unsatisfactory performance and, hence, reduce the hesitation of practitioners to use such techniques in practice. The stability of the Muar embankment is analyzed probabilistically and deterministically at various stages during construction (i.e. different embankment heights). Four embankment heights are considered; 2.5, 3.3, 3.5 and 4.0 m. The probabilistic analyses are conducted following the same approach described previously. Figure 8 shows the variation of the probability of unsatisfactory performance and factor of safety with embankment height. The plot indicates little increase in the probability of unsatisfactory performance up to a height of about 3.3 m followed by a sharp increase in probability value as the embankment height exceeds 3.5m.

Based on the observed field performance of the Muar embankment and typical factors of safety used in practice, a 3.3 m high embankment (a deterministic factor of safety of 1.42) would have been anticipated to perform adequately in a conventional slope assessment. Probabilistic slope stability analysis of this embankment indicates a mean factor of safety of 1.42 with a 0.20 standard deviation. The probability of unsatisfactory performance is $1.38\text{x}10^{-2}$, and the reliability index is 2.07. For comparison, the probability of unsatisfactory performance and the reliability index of the failed embankment (4.7 m in height) are $24.1\text{x}10^{-2}$ and 0.72, respectively.

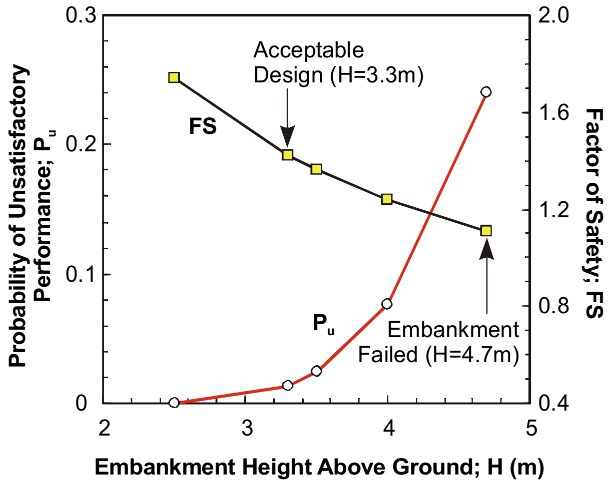

Figure 8 Variation of the probability of unsatisfactory performance and the factor of safety with embankment height.

4.6 Impact of Autocorrelation Distance

The sensitivity of the estimated probability of unsatisfactory performance of the 3.3 m high embankment to the value of the autocorrelation distance, r_o, is investigated by repeating the probabilistic analysis using different autocorrelation distances. Five autocorrelation distances within the postulated range of 5 to 15 m (Section 4.2) are considered. The probabilities of unsatisfactory performance range between 1.1×10^{-2} for r_o=5 m, and 1.7×10^{-2} for r_o=15 m. From a practical perspective, the probability of unsatisfactory performance of the Muar embankment does not seem to be sensitive to the autocorrelation distance of the marine clay foundation. Addressing the stability of a tailings dyke on a marine clay shale foundation, El-Ramly et al. (2003) noted a similar conclusion.

4.7 Sensitivity Analysis

Using @Risk software, a sensitivity analysis is undertaken to assess the relative contributions of input variables to the uncertainty in the factor of safety. Spearman rank correlation coefficient is used as the analysis tool. It measures the strength of linear correlations between input variables and the factor of safety. Its numeric value ranges between 1 and –1. A value of 1 indicates a perfect positive correlation, a value of –1 indicates a perfect negative correlation, and zero indicates no correlation. Figure 9 shows Spearman rank correlation coefficients for all input variables.

The plot indicates that the impact of the uncertainty in Bjerrum's vane correction factor on the reliability of the computed factor of safety is significant, and comparable to that of the spatial variability of the undrained shear strength. In other words, the use of Bjerrum's factor has introduced an additional element of uncertainty that is as significant as the inherent spatial variability of the undrained shear strength. This highlights the drawbacks of using empirical factors and correlations without proper understanding of their limitations and, more importantly, their reliability. The plot also shows that the uncertainty in the contribution of fill strength to stability has a large impact on the reliability of the factor of safety; a longstanding issue still facing practitioners in the design of embankments on soft soils.

In conventional slope design practice, deterministic estimates of the above two quantities, namely; the reduction (if any) in the measured vane strength and the contribution of fill strength to stability, ought to be made. These estimates are largely subjective and depend on the designer's judgement and experience, which explains, at least in part, the significant scatter in the predictions of embankment height at failure in Figure 1.

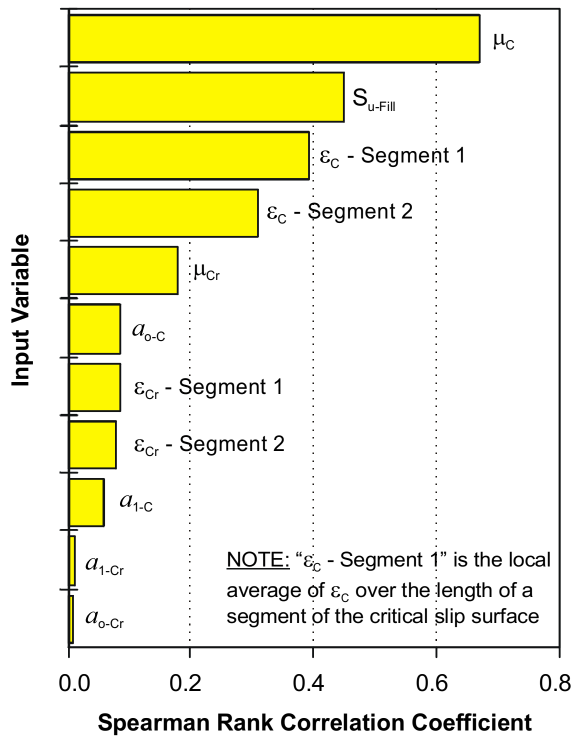

Figure 9 Spearman rank correlation coefficients between input variables and factor of safety

As expected, the uncertainty in the strength of the weathered clay crust has a small impact on the reliability of the computed factor of safety. Because of the relatively large number of field vane measurements, the statistical uncertainty in the mean trend of the undrained shear strength of the soft clays also has a minimal impact on the analysis.

5. CONCLUDING REMARKS

In a similar study, El-Ramly et al. (2002b) conducted a probabilistic slope analysis of the Lodalen slide. Based on a back analysis of the failure, they redesigned the cut slope (hypothetically) to a flatter inclination deemed stable and undertook a probabilistic assessment of its stability. In another study, El-Ramly et al. (2003) presented a probabilistic analysis of a tailings dyke on a pre-sheared clay-shale foundation. The dyke performance was monitored during and after construction and is deemed adequate. Table 3 summarizes the results of the two case studies together with the results of the Muar embankment at an intermediate height, 3.3 m, deemed stable.

Table 3. Safety indices of three case histories

Soil Layer	E[FS]	σ[FS]	P_u	β
Lodalen Slope	1.33	0.07	≈ 0.00	4.85
Tailings Dyke	1.31	0.14	$0.16x10^{-2}$	2.31
Muar Embankment	1.42	0.20	$1.38x10^{-2}$	2.07

The results in Table 3 indicate two important observations. First, the probabilities of unsatisfactory performance of adequate slopes appear to be much higher than some of the recommendations reported in the literature. For example, the US Corps of Engineers (1995) recommended a probability of unsatisfactory performance of $3x10^{-5}$ or a minimum reliability index of 4.0 as design targets for a “Good” performance level. Second, the factor of safety of the Muar embankment is higher than those of the two other cases, yet its probability of unsatisfactory performance is substantially higher. This inconsistency is attributed to the significant uncertainties in the analysis of the Muar embankment, including Bjerrum’s vane correction factor and embankment strength. Neither of these issues would be addressed in conventional slope stability analyses based on the deterministic factor of safety.

REFERENCES

Aas, G., Lacasse, S., Lunne, T., and Hoeg, K. 1986. Use of in situ tests for foundation design on clay. In Use of in Situ Tests in Geotechnical Engineering, Proceedings of In Situ’86. Geotechnical Special Publication No. 6, ASCE, Blacksburg, USA, June 23-25, pp 1-30.

AIT, 1989. Laboratory test data on soil samples from the Muar flats test embankment. Asian Institute of Technology. Research Report – Phase II

Bishop, A.W. 1955. The use of the slip circle in the stability analysis of slopes. Geotechnique, 5(1): 7-17.

Bjerrum, L. 1972. Embankments on soft ground. Proceedings of ASCE Specialty Conference on Performance of Earth and Earth-Supported Structures. Purdue University, Lafayette, USA, June 11-14. Volume 2. pp 1-54.

Bjerrum, L. 1973. Problems of soil mechanics and construction on soft clays. Proceedings of 8th International Conference on Soil Mechanics and Foundation Engineering. Moscow. Volume 3. pp 111-159.

Brand, E.W., and Premchitt, J. 1989. Comparison of the predicted and observed performance of the Muar test embankment. Proceedings of the Symposium on Trial Embankments on Malaysian Marine Clays. Kuala Lumpur, Malaysia, November. Volume 3.

El-Ramly, H. 2001. Probabilistic analyses of landslide hazards and risks: Bridging theory and practice. Ph.D. thesis, University of Alberta, Canada.

El-Ramly, H., Morgenstern, N.R., and Cruden, D. 2002a. Probabilistic slope stability analysis for practice. Canadian Geotechnical Journal, 39: 665-683.

El-Ramly, H., Morgenstern, N.R., and Cruden, D. 2002b. Probabilistic Stability Analysis of Lodalen Slide. Proceedings, 55th Canadian Geotechnical Conference, Niagara Falls, Canada, October 20-23. Canadian Geotechnical Society, pp 1053-1060.

El-Ramly, H., Morgenstern, N.R., and Cruden, D. 2003. Probabilistic stability analysis of a tailings dyke on presheared clay-shale. Canadian Geotechnical Journal, 40: 192-208.

Ferkh, Z., and Fell, R. 1994. Design of embankments on soft clay. Proceedings of 13th International Conference on Soil Mechanics and Foundation Engineering, New Delhi, India, January 5-10. Volume 2. pp 733-738.

Hassan, A., and Wolff, T. 1999. Search algorithm for minimum reliability index of earth slopes. Journal of Geotechnical and Geoenvironmental Engineering, ASCE, 125(4): 301-308.

Kay, J.N. 1993. Probabilistic design of foundations and earth structures. In Probabilistic Methods in Geotechnical Engineering, Li & Lo (eds.). Balkema, Rotterdam. pp 49-62.

Lefebvre, G., Pare, J.J., and Dascal, O. 1987. Undrained shear strength in the surficial weathered crust. Canadian Geotechnical Journal, 24: 23-24.

Microsoft, 1997. Microsoft Excel 97. Microsoft Corporation, Redmond, Washington, USA.

Palisade Corporation, 1996. @Risk: risk analysis and simulation add-in for Microsoft Excel or Lotus 1-2-3. Palisade Corporation, Newfield, NY, USA.

Poulos, H.G., Lee, Y.C., and Small, J.C. 1990. Predicted and observed behaviour of a test embankment on Malaysian soft clays. Research Report No. R620, University of Sydney.

Vanmarcke, E.H. 1977. Probabilistic modeling of soil profiles. Journal of the Geotechnical Engineering Division, ASCE, 103(11): 1227-1246.

US Army Corps of Engineers 1995. Introduction to Probability and Reliability Methods for Use in Geotechnical Engineering. Engineering Technical Letter No. 1110-2-547, Washington DC.

Vanmarcke, E.H. 1983. Random fields: analysis and synthesis. MIT Press, Cambridge, Massachusetts, USA.